Monolithic Polarization Controller on Regrowth-Free InGaAsP/InP Platform with Strained MQW Layer

Maiko Ito, Kosuke Okawa, Takahiro Suganuma, Takuo Tanemura, and Yoshiaki Nakano
School of Engineering, The University of Tokyo, 7-3-1 Hongo, Bunkyo-ku, Tokyo, 113-8656, Japan
m.ito@hotaka.t.u-tokyo.ac.jp

Abstract: Carrier-injection-based polarization controller with strained MQW layer is demonstrated. Based on novel design concept, both polarization-rotating and phase-shifting sections are integrated monolithically on regrowth-free InGaAsP/InP platform to achieve efficient conversion over the entire Poincaré sphere.

OCIS codes: (130.3120) Integrated optics devices; (230.4205) Multiple quantum well (MQW) modulators;

1. Introduction

Electrically tunable high-speed polarization controller will be an essential component in wide ranges of applications, such as DSP-free coherent communication [1], polarization-based microwave photonics [2], and polarization-encoded quantum key distribution [3]. In particular, monolithically integrated polarization controllers are highly desired to achieve significant reduction in size, cost, and power consumption.

Among various types of integrated polarization controllers demonstrated on silicon and InP platforms [3-9], those based on a straight-line waveguide configuration [6-9] are attractive due to the simplicity and compactness. By cascading multiple stages of polarization converter (PC) and polarization-dependent phase shifter (PD-PS) sections, conversion to arbitrary state of polarization (SOP) can be achieved [7]. In this scheme, the electrically tunable PD-PS plays an important role to provide required phase offset between the transverse-electric (TE) and transverse-magnetic (TM) components. For efficient operation, use of a strained multiple-quantum-well (MQW) active layer is effective due to the large inherent birefringence, which can be tuned upon current injection. On the other hand, such MQW structure is generally unfavorable at the PC section. In the previous demonstration, therefore, butt-joint active-passive integration technique had to be used to insert MQW stack only in the PD-PS section [8].

In this work, we demonstrate all-active polarization controller with a compressively strained MQW active layer fabricated on a regrowth-free InGaAsP/InP platform, which attains both the high tuning efficiency and the simple fabrication process. Using the optimally designed and fabricated device, efficient conversion of the SOP over the entire Poincaré sphere is demonstrated with a total current of less than 40 mA.

2. Operating principle of integrated MQW polarization controller

Figure 1 illustrates the schematic of the monolithic polarization controller considered in this work, comprising the PC and PD-PS sections in a straight-line configuration. As shown in Fig. 1(b), the PC section has an asymmetric cross-section and is used to provide a fixed rotation to the Stokes vector (SV) on the Poincaré sphere. On the other hand, the PD-PS section has a symmetric cross-section as shown in Fig. 1(c), and enables tunable rotation of the SV around the S_1 axis under an external electrical control signal. By cascading two stages of these PC and PD-PS sections, we can convert input TE or TM light into an arbitrary SOP at the output [7].

For efficient operation of the polarization controller, PD-PS needs to have large phase difference between the TE and TM modes when an electrical bias is applied. To this end, use of compressively strained MQW active layer is effective. Due to the splitting of the heavy-hole (HH) and light-hole (LH) energy levels in a strained MQW, large polarization-dependent band-filling effect can be obtained under current injection [8]. On the other hand, such MQW layer is generally unfavorable at the PC section, since it hinders necessary fixed polarization rotation. Here, however, we demonstrate that by properly adjusting the waveguide structure at the PC section, necessary polarization rotation can be obtained even with the MQW layer, thus avoiding the need for costly active-passive integration.

As the light propagates through the PC section, its SV rotates about a birefringence vector $\mathbf{\Omega} = (\beta_1 - \beta_2)[\cos(2\psi), \sin(2\psi), 0]^{\mathrm{T}}$ by an angle $|\mathbf{\Omega}|L$, where L is the length of PC, β_1 and β_2 are the propagation constants of the two eigenmodes of the asymmetric waveguide, and ψ represents the effective tilt angle of these eigenmodes as illustrated in Fig. 1(b). In order to realize a perfect polarization controller that can convert input TE light into an arbitrary SOP, the SV after the first PC [PC1 in Fig. 1(a)] needs to lie on the S_2-S_3 plane. We can understand from Fig. 1(b) that such condition can only be satisfied if the vector $\mathbf{\Omega}$ is located inside the gray shaded region in Fig. 2, or in other words, if ψ is in the range between 22.5° and 67.5°.

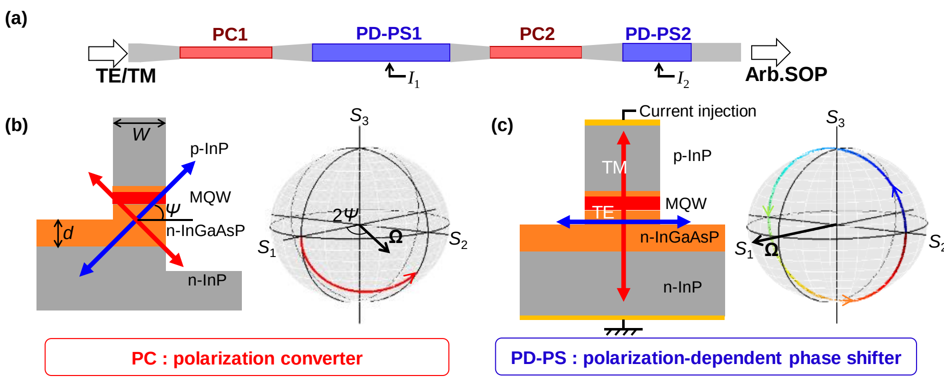

Fig. 1 Schematic of the monolithic polarization controller on InP with strained MQW: (a) the entire structure, (b) PC section, and (c) PD-PS section. As the light propagates inside respective waveguides, its Stokes vector rotates about $\mathbf{\Omega}$ on the Poincaré sphere.

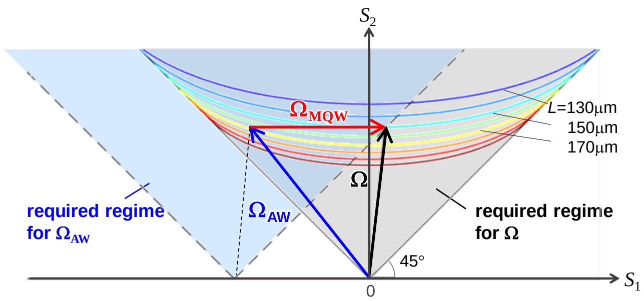

Fig. 2 Required regimes for $\mathbf{\Omega}$ and $\mathbf{\Omega}_{AW}$ on the S_1-S_2 plane to achieve polarization conversion over the entire Poincaré sphere.

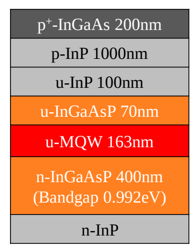

	well	barrier
Material	13 × InGaAsP	14 × InGaAsP
Thickness	5 nm	7 nm
Bandgap	0.827 eV	1.127eV
Strain	+0.8% (Compressive)	-0.3% (Tensile)

Fig. 3 Epitaxial layer profile of the device.

When a birefringent MQW layer is inserted inside the asymmetric waveguide, the birefringence vector $\mathbf{\Omega}$ can be expressed as $\mathbf{\Omega} \equiv \mathbf{\Omega}_{\mathrm{AW}} + \mathbf{\Omega}_{\mathrm{MQW}}$, where $\mathbf{\Omega}_{\mathrm{AW}}$ represents the SV rotation induced by the pure asymmetric geometry of the waveguide, while the additional vector $\mathbf{\Omega}_{\mathrm{MQW}}$ accounts for the intrinsic birefringence of the MQW layer. Since MQW exhibits a refractive index difference between the TE and TM modes, $\mathbf{\Omega}_{\mathrm{MQW}}$ is parallel to the S_1 axis. As a result, the required regime for $\mathbf{\Omega}_{\mathrm{AW}}$ is shifted by $\mathbf{\Omega}_{\mathrm{MQW}}$ as indicated by the blue shaded region in Fig. 2. If $|\mathbf{\Omega}_{\mathrm{MQW}}|$ is small enough, we can design the asymmetric waveguide cross-section of the PC section, so that $\mathbf{\Omega}_{\mathrm{AW}}$ lies inside the blue required region shown in Fig. 2.

3. Device design

We first optimized the MQW stack of the active layer to maximize the tuning efficiency under current injection, while keeping the absorption below an acceptable level. From a detained numerical analysis, we determined the epitaxial layer structure as shown in Fig. 3. In order to keep $|\mathbf{\Omega}_{\mathrm{MQW}}|$ within an acceptable level, the offset-QW design was selected, where the strained InGaAsP/InGaAsP MQW active layer was located on the top of bulk InGaAsP core layer to have modest confinement. The MQW layer was designed properly to exhibit the absorption edges for the TE and TM modes at around 1400 nm and 1300 nm, respectively, so that large polarization-dependent phase shift can be obtained at 1550 nm wavelength.

Once the epitaxial layer design was fixed and $\mathbf{\Omega}_{\mathrm{MQW}}$ was obtained, target $\mathbf{\Omega}_{\mathrm{AW}}$ was decided as shown in Fig. 2 so that the total birefringence vector $\mathbf{\Omega}$ comes to the center of the required regime (indicated by gray shaded region in Fig. 2). Then, eigenmode analysis based on the finite-element method was carried out to search for the optimal values of W and d in Fig. 1(b) to achieve the target $\mathbf{\Omega}_{\mathrm{AW}}$. As a result of these optimization procedures, we selected W to be 1060 nm and d to be 375 nm, from which L was determined to be 150 μm. As for the PD-PS sections, waveguide width and length at PD-PS1 were set to be 2.5 μm and 2 mm, respectively. The length of PD-PS2 was reduced to 1 mm, since only π phase shift is required at PD-PS2.

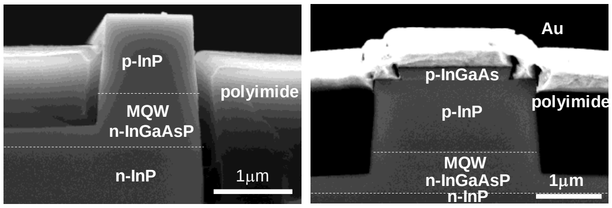

(a) (b)

Fig. 4 Cross-sectional SEM images at (a) PC and (b) PD-PS sections of the fabricated device.

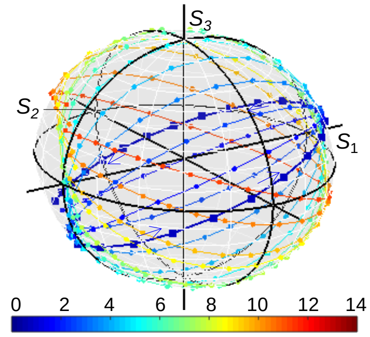

Fig. 5 Measured output SV under current injection.

4. Device fabrication and measurement

The designed device was fabricated by a simple regrowth-free process. The asymmetric waveguides at the PC sections were formed by a self-aligned dry-etching process based on an angled electron-beam evaporation [10]. After passivation with SiO_2 layer and planarization using polyimide, top and bottom Ti/Au contacts were formed. Figure 4 shows the cross-sectional scanning-electron microscope (SEM) images of the fabricated device.

The device was mounted and characterized at a room temperature. In order to avoid the effects of reflection at the device facets, we employed an incoherent light source at 1550-nm wavelength with the 3-dB bandwidth of 2 nm, which was generated by spectrally slicing the amplified spontaneous emission from an erbium-doped fiber amplifier using an arrayed-waveguide grating [10]. The light was polarized to TE mode by using a polarizer followed by a half-wave plate and a quarter-wave plate and incident to the device through a lensed fiber. The SOP of the output light from the device was measured by a polarization analyzer.

Figure 5 shows the measured output SV on the Poincaré sphere. When the current to PD-PS1 varies from 0 to 26 mA, the output SV rotates around a circular trajectory represented by the dark blue squares. Next, as the current to PD-PS2 is increased from 0 to 14 mA, the entire circular trajectory rotates as indicated by the different colors in Fig. 5. As a result, we can see that nearly entire surface of the Poincaré sphere is covered by adjusting the injection current to PD-PS1 and PD-PS2.

5. Conclusions

We have designed, fabricated, and demonstrated a carrier-injection-based polarization controller with a strained MQW layer on a regrowth-free InGaAsP/InP platform. By using novel design concept to optimize the waveguide structure with a birefringent MQW layer at the PC section, both polarization-rotating and phase-shifting sections were integrated monolithically on a compact InP chip. Using the fabricated device, efficient conversion of SOP over the entire Poincaré sphere was demonstrated with a total current of less than 40 mA.

Acknowledgement: This work was financially supported by the Grant-in-Aid of Japan Society for the Promotion of Science.

References

[1] J. K. Perin, et al., "Design of low-power DSP-free coherent receivers for data center links," J. Lightw. Technol., **35**, 4650 (2017).
[2] Y. Zhang and S. Pan, "Broadband microwave signal processing enabled by polarization-based photonic microwave phase shifters," J. Quantum Electron., **54**, 0700112 (2018).
[3] C. Ma, et al., "Silicon photonic transmitter for polarization-encoded quantum key distribution," Optica, **3**, 1274 (2016).
[4] W. D. Sacher, et al., "Polarization rotator-splitters and controllers in a Si_3N_4-on-SOI integrated photonics platform," Opt. Exp., **22**, 11167 (2014).
[5] P. Dong, et al., "128-Gb/s 100-km transmission with direct detection using silicon photonic Stokes vector receiver and I/Q modulator," Opt. Exp., **24**, 14208 (2016).
[6] B. M. Holmes, et al., "A semiconductor laser with monolithically integrated dynamic polarization control," Opt. Exp., **20**, 20545 (2012).
[7] Y. Kawabata, et al., "Proposal and experimental demonstration of monolithic InP/InGaAsP polarization modulator," in Proc. Eur. Conf. Opt. Commun. (ECOC), Mo.3.C.2. (2014).
[8] M. Kazi, et al., "High-speed carrier-injection-based polarization controller with InGaAlAs/InAlAs multiple-quantum wells," IEEE Photon. Technol. Lett., **29**, 1951 (2017).
[9] J. Sarmiento-Merenguel, et al., "Demonstration of integrated polarization control with a 40 dB range in extinction ratio," Optica, **2**, 1019 (2015).
[10] M. Zaitsu, et al., "Experimental demonstration of self-aligned InP/InGaAsP polarization converter for polarization multiplexed photonic integrated circuits," Opt. Exp., **21**, 6910 (2013).